Boundary-Layer Meteorol (2007) 122:293–320
DOI 10.1007/s10546-006-9116-y

ORIGINAL PAPER

Experimental study of the transfer velocity for urban surfaces with a water evaporation method

Ken-ichi Narita

Received: 19 May 2005 / Accepted: 24 July 2006 /
Published online: 21 October 2006

Abstract A major problem in urban climate modelling is determining how the heat fluxes from various canyon surfaces are affected by canyon flow. To address this problem, we developed a water evaporation method involving filter paper to study the distribution of the convective transfer velocity in urban street canyons. In this method, filter paper is pasted onto a building model and the evaporation rate from the paper is measured with an electric balance. The method was tested on 2D (two-dimensional) street canyon models and 3D model arrangements. Moreover, in this technique, it is easy to restrict the flux within an arbitrary surface in question. That is, the evaporation distribution on a surface can be studied by using several small pieces of filter paper. In the 2D case, the wall transfer velocity was strongly dependent on the canyon aspect ratio for perpendicular wind directions and it varied widely with height within both windward and leeward wall surfaces. For 3D cubic arrays, the relation to canyon aspect ratio was largely different from that of the 2D canyon. And, as a case study, the variation of wind direction was investigated for a city-like setting. The area-averaged transfer velocity was insensitive to wind direction but its local deviation was significant. Finally, we measured the transfer velocity for a clustered block array surrounded by relatively wide streets. The effect of spatial heterogeneity on the transfer velocity was significant. Moreover, for a fixed total building volume, the transfer velocity was considerably larger when the building height varied than when it was uniform. Therefore, the water evaporation method with filter paper is expected to be useful for studying the transfer velocity and ventilation rates in urban areas with various canyon shapes.

Keywords Sensible heat flux · Spatial heterogeneity · Turbulent transfer · Urban canopy layer · Urban climate

K. Narita (✉)
Department of Engineering, Nippon Institute of Technology, 4-1 Gakuen-dai, Miyashiro, Saitama, 345-8501, Japan
e-mail: narita@nit.ac.jp

1 Introduction

An urban area can be considered as a collection of buildings of various shapes and sizes. In the mesoscale modelling of urban climate, the effects from the buildings (roughness elements) have been treated using parameters such as the roughness length and displacement height. Such a parameterization is convenient for city-scale considerations; however, the surface fluxes do not depend on the specific surface morphology. Moreover, it is difficult to evaluate urban mesoscale models because it is difficult to define the air temperature that should be compared to measurements.

To simulate the heat balance of an urban area in detail, one should know the turbulent transfer from all active surfaces as well as the radiative fluxes. Recent urban canopy models, such as Masson's (2000) TEB (Town Energy Balance) model, express the turbulent transfer as a network of resistances between the air and surface. However, there are very few studies that provide values of these resistances (or transfer velocity) for urban surfaces; therefore, the parameterization of these processes has been empirical or based only on the drag determined from vertical wind profiles above a series of street canyons (Kusaka et al. 2001; Martilli et al. 2002). Comparisons with field data have been partially performed (Masson et al. 2002), however systematic validation of dynamic processes has been required particularly for turbulent fluxes.

Among the experimental studies of the convective transfer velocity on outside building surfaces, few are full-scale measurements (Ito et al. 1972; Cole and Sturrock 1977; Loveday and Taki 1996; Clear et al. 2003; Hagishima and Tanimoto 2003). Since the results varied considerably, understanding the behaviour of the transfer velocity remains controversial. In addition, Kanda et al. (2005) used the heat balance method on a scale-model field experiment with regular cubic arrays to study heat transfer from urban surfaces. The most relevant, systematic dataset, though it is restricted to the 2D canyon case, is from Barlow et al. (2004) in which the naphthalene sublimation technique was used in wind-tunnel model experiments. The naphthalene sublimation technique (Goldstein and Cho 1995) is a standard method for determining the mass transfer velocity. Since the 1940s, it has been used to determine heat transfer coefficients and it has been particularly useful for relatively complex shapes. This technique relies on the heat-mass transfer analogy known as the Lewis relation. In the case of similar experiments about heat transfer, a range of heat fluxes need to be considered: for example, the conductive flux to the ground or the radiative flux between facing surfaces, as well as the convective heat flux from the objective surface. Such mass transfer methods measure the convective flux directly from the arbitrary surface in question, which means they have an advantage of deducing the precise transfer velocity readily.

This paper describes a method involving water evaporation from filter paper to measure the convective fluxes from urban surfaces. Compared with the use of naphthalene, water is easy to handle and water vapour has no odour and no toxicity. First, we used the method to systematically study the transfer velocity from each surface in periodic 2D (two-dimensional) canyons and cubic arrays. Such simple, periodic structures are useful for parameterization of canopy models, but real cities have more complex structures. Therefore, we also studied the dependence of the transfer velocity on wind direction in 3D city-like settings and finally we also investigated heterogeneous three-dimensional structures.

2 The water evaporation technique using filter paper

The basic building model is a hollow box made of acrylic resin 1-mm thick (Fig. 1). We pasted filter paper onto this model surface and moistened it sufficiently but not so much that it drips. This wetted model was set in a wind tunnel for a half hour, and the weight loss during this period was measured using an electric balance (resolution 0.1 mg). The filter paper was 1 mm thick, and its side surfaces were treated with a waterproofing agent. A fine thermistor sensor having a diameter of 1 mm was inserted from the side surface just below the paper surface to measure evaporating surface temperature. During the weighing, the building model sample was packed in an airtight plastic bag. The total weight of the model was about 0.035 kg, and the weight loss was typically about 200–700 mg. Then the mass transfer velocity (W_t) was calculated as

$$W_t = E/(\rho_s - \rho_a), \tag{1}$$

where E is the evaporation rate, ρ_s is the saturated water vapour density at evaporating surface temperature, and ρ_a is the vapour density of the incoming flow. The evaporation rate should be constant and thus the evaporating surface remains saturated throughout an experiment. If the model surface were to partially dry out, the surface temperature would rise quickly, and as the surface temperature was monitored during an experiment, we could thus determine if a filter paper dried out. According to the preliminary examination, this occurs when the total evaporation amount exceeds 0.56 kg m^{-2}; namely about 0.002 kg weight loss in the 60 mm by 60 mm sample. Since actual values in the experiments were far lower than this criterion, no case was omitted.

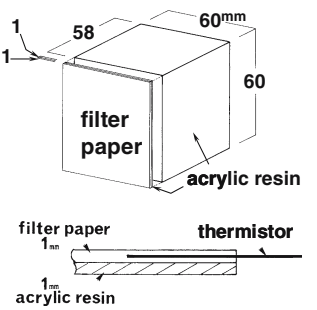

Fig. 1 Building model for the water evaporation technique. The filter paper and the acrylic resin were each 1-mm thick

Experiments were carried out in an open-circuit wind tunnel at Hiroshima University (Fig. 2); the outlet is 900 mm high and 1800 mm wide. The roughness elements were L-shaped aluminium plates 1800 mm long. There is no wall and ceiling in the roughness-setting area and working section. Figure 3 shows the vertical profiles of mean wind speed and turbulence intensity (T_I) at the upstream edge of the working section, measured with a single hot wire anemometer (5 μm in diameter) that had been calibrated against a Pitot-static tube. Sampling frequency is 20 Hz. The best fit of the logarithmic law gives a roughness length (z_0) of 4.9 mm, and the displacement height was assumed to be zero. The value of T_I at the model roof level (60 mm) was about 20%. This figure shows that the depth of the boundary layer was about five

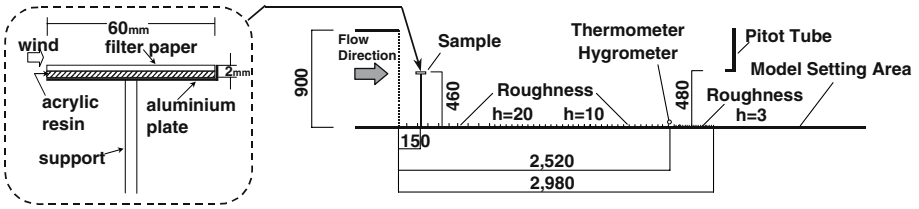

Fig. 2 Side view of the wind-tunnel apparatus. The reference measurement is detailed on the left and the building model was put on the right side. The filter paper and aluminium plate were both 60 mm wide, tunnel dimension in the direction into the page is 1800 mm and the roughness elements were L-shaped aluminium plates 1800 mm long

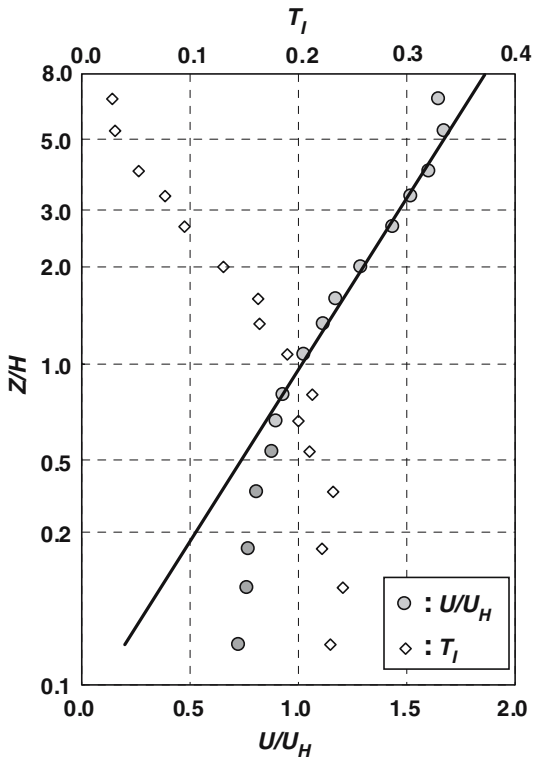

Fig. 3 Profiles of the mean wind speed and the turbulence intensity T_I in the model setting area. U_H is the mean wind speed at the representative model height $H(= 60\,\text{mm})$

times the building height. At the top of the boundary layer, the wind speed was fixed at $4\,\text{m}\,\text{s}^{-1}$ except where otherwise stated. The Reynolds number based on this wind speed and building height is 16,000. For the lower wind speed at the building height, the Reynolds number is about 10,000. In the following experiments, this profile measuring point corresponds to the model position for the single model case and to the upstream first array position for cyclic arrangement cases.

The incoming air temperature and humidity were not controlled; nevertheless, the temperature and relative humidity of the incoming air were measured using a thermistor and capacitive hygrometer just upstream of the model. Measurements were recorded at 1 Hz. The change of ρ_a due to the evaporation from wetted samples

is negligible because the incoming flow is sufficiently mixed with ambient room air through the open-circuit. In each run, we measured the evaporation rate from a reference sample in the form of a horizontal plate in the free stream simultaneously (left side of Figure 2).

The heat-mass transfer analogy requires that the ratio of mass to heat diffusivity be of order 1. Water vapour satisfies this criterion because $Sc = 0.61$ and $Pr = 0.71$. However, the large latent heat of evaporation for water is a disadvantage for the experiments. In the case of naphthalene, the heat of sublimation is small enough so that surface temperature can be taken as equal to air temperature and the background vapour density is negligible. Therefore, measurements of both surface temperature and background vapour density are required in the water evaporation method.

Because there is no effective heat source to offset the evaporative cooling except for convective heat flux from air to the surface, the surface of the wet sample cools to a temperature below that of the ambient air. To avoid a large time variation of the surface temperature during an experiment, the wetted sample was set at the experimental position in the wind tunnel so as to cool down before the initial weighing. The relation between the air-surface temperature difference and the evaporation rate is shown in Fig. 4a on the reference sample. The magnitude of the temperature difference increases approximately linearly with an increase of the evaporation rate. In this figure, the simulated surface temperature, assuming that the latent heat flux of evaporation is balanced by the convective heat flux from air to the surface, is also plotted for some typical air temperature conditions. Here, it was assumed that the heat transfer velocity is equal to that of mass transfer. Measured surface temperature was slightly higher than the simulated value. This discrepancy is partly because of the conductive heating from the base plate and radiative heating from ambient air, but the precise contribution of these factors is not clear.

By adopting such an assumption of surface heat balance, we can estimate the experimental error for this water evaporation method. Table 1 is the result of a sensitivity analysis for each measured term in various air temperature and humidity conditions. The relative error on transfer velocity becomes larger in high humidity conditions. Therefore, we performed the experiment for relative humidity lower than 60%.

Judging from the accuracy of used instruments, the largest uncertainty in the transfer velocity is from the relative humidity measurement in the incoming flow. Therefore, the capacitive humidity sensor was frequently calibrated using several sealed bottles containing saturated aqueous solution of chemicals such as lithium chloride (LiCl) and potassium sulphate (K_2SO_4). Another factor that can produce errors is temperature gradients on the measured surface. We used an infrared thermograph to check the surface temperature distribution within a sample filter paper and found that the temperature varied by about 0.1 K, which is much larger than the thermistor accuracy. Thus, thermograph measurements in every experiment would be ideal; however this was not done because it is technically difficult, particularly for a wall surface in a dense arrangement.

The variation in measured values on the reference sample in Fig. 4b shows the typical experimental uncertainty. This plot shows the transfer velocity at reference point W_{t_0}, which will be used to normalize the results on the model. The systematic tendency is that W_{t_0} slightly decreases as the evaporation rate increases. Including this tendency, the relative standard error of W_{t_0} is 4.1%. To help reduce variations in the data, each value measured on the model is normalized by the reference value (W_{t_0}) that was obtained at the same time.

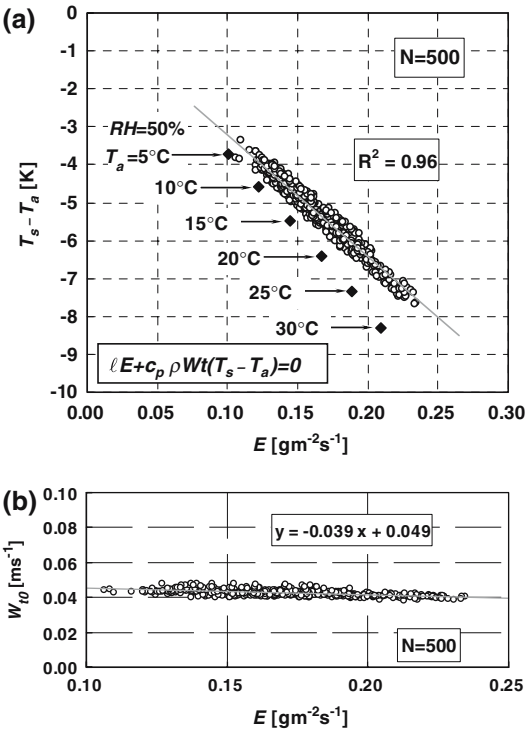

Fig. 4 (**a**) Surface temperature drop $T_s - T_a$ and evaporation rate E on the reference plate. The closed diamond symbols are the simulated values provided that latent heat flux for evaporation is balanced convective heat flux from air to the surface. In the formula, ℓ is the latent heat of evaporation for water and $c_p \rho$ is heat capacity of the air. (**b**) Transfer velocity of the reference plate W_{t_0} for various air temperatures and humidities. The number of data points is 500 and wind speed was 4 m s^{-1}

Table 1 Sensitivity analysis on experimental error (in%) of the transfer velocity with a water evaporation method

Air Temp.	Errors	RH = 30%	40%	50%	60%	70%
10°C	Surface Temp. 0.1°C	1.2	1.5	2.0	2.6	3.7
	Air Temp. 0.1°C	0.5	0.8	1.3	1.9	3.0
	Relative Humidity 0.5	1.4	1.7	2.0	2.5	3.4
20°C	Surface Temp. 0.1°C	1.3	1.7	2.3	3.1	4.5
	Air Temp. 0.1°C	0.7	1.0	1.6	2.4	3.8
	Relative Humidity 0.5	1.9	2.2	2.7	3.4	4.6
30°C	Surface Temp. 0.1°C	1.5	2.0	2.7	3.8	5.7
	Air Temp. 0.1°C	0.8	1.3	2.0	3.1	5.0
	Relative Humidity 0.5	2.5	3.0	3.7	4.7	6.5

3 Scale effects and Reynolds number dependence

Before describing the main results for urban-like settings, the scale effects should be considered. In this kind of scalar flux measurement from a scale model, the magnitude of the flux should depend on the sample size even if the flow characteristics around the sample are kept constant. Such a scale dependency of the scalar flux is sometime called an "edge effect" or "oasis effect". For a flat plate, the dimensionless number for the mass transfer velocity (W_t), the Sherwood number $Sh(= W_t X/D$ with D the molecular diffusivity and X a representative length; here, the length from leading edge)

$$Sh = ARe^m Sc^n, \tag{2}$$

where Re is the Reynolds number ($= UX/\nu$ with U wind speed and ν the coefficient of kinematic viscosity), and Sc is the Schmidt number ($= \nu/D$). For turbulent conditions, $m = 4/5$ and $n = 1/3$ have been proposed, and the value of A is typically 0.0296 for the local Sh but 0.037 for an integral surface Sh(Incropera and DeWitte 1996).

To check the scale effect for this method, we measured the transfer velocity of a 300 mm by 240 mm horizontal plate in the beginning. As shown in Fig. 5, the distribution of local transfer velocity along the stream direction was measured using a sample 10-mm long (along the streamwise direction) for wind speeds of 1.5 and 4.5 m s^{-1}. The entire plate was wetted. If $m = 4/5$ in Eq. (2), the transfer velocity would decrease with the $-1/5$ power of the distance from the leading edge. For both wind speeds, the data agree with this scaling relation, and means that the transfer velocity has a scale effect and the exponent on the Reynolds number in Eq. (2) is 4/5. In practice, the variation in W_t is noticeable within about 100 mm from the leading edge, but it becomes relatively small further downstream.

Does the scale effect also exist for the vertical surface? To examine this question, we measured the wall surface transfer velocity with cubic models in several sizes. The dimensions of prepared models were 30, 45, 60, 75, and 90 mm. If the Sherwood number is proportional to the 4/5 power of the Reynolds number, the transfer velocity should be also proportional to 4/5 power of the wind speed. To make this point clear, these measurements were performed at several different values of wind speed.

Figure 6 shows the relations between the transfer velocity and the model dimension for a wind speed of 4 m s^{-1}. These values were estimated from the regression curves in each model size as shown in Fig. 7. The roof has the highest transfer velocity, followed by the windward wall, the side wall, and then the leeward wall in all cases. Although the tested range was limited by the boundary-layer depth, the transfer velocity of all surfaces decreased with increasing model dimension to the $-1/5$ power, in good

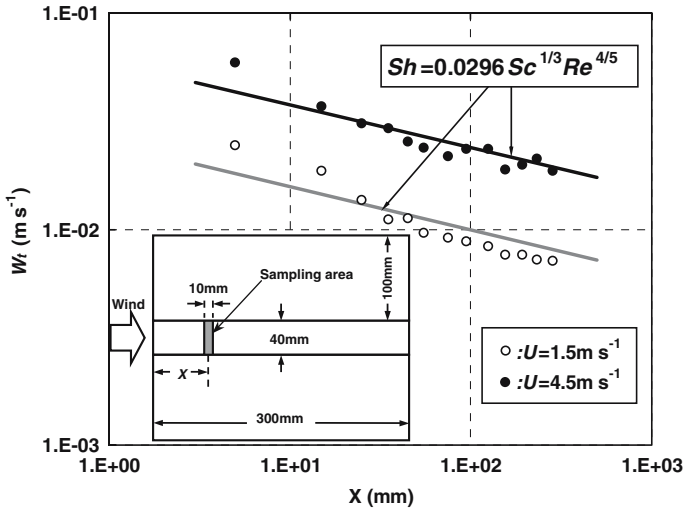

Fig. 5 Local transfer velocity along the stream direction on the small sampling area within the (300 × 240 mm) horizontal plane surface sketched in the upper right. The Reynolds number Re is based on the length X from the leading edge of the wet surface

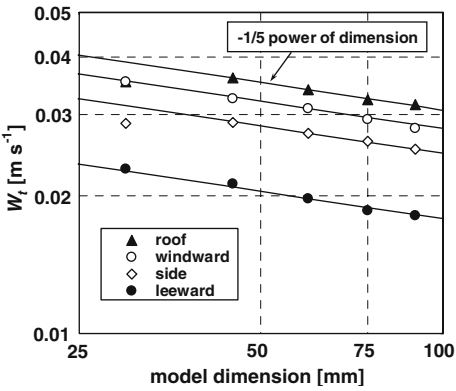

Fig. 6 Transfer velocity for surfaces on a single cubic model for various model heights. The wind speed was 4 m s^{-1}

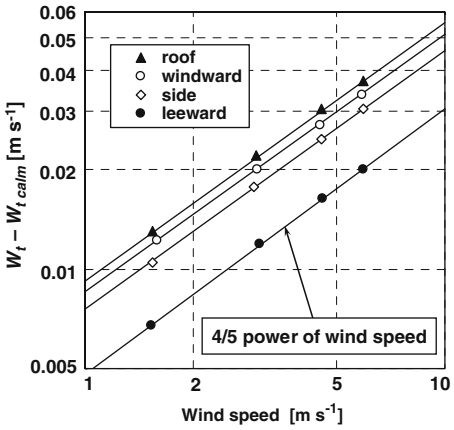

Fig. 7 Transfer velocity for single cubic model surfaces at various wind speeds. The cube size is 60 mm and the solid curves are wind speed to the 4/5th power

agreement with the scaling law. As shown in Figure 3, the vertical profile of wind speed deviated from the logarithmic law in the bottom part of the boundary layer. Beside, regarding the smaller model case, the Reynolds numbers was not sufficient in comparison with the criterion of 10,000. These are likely the main reasons that the minimum dimension model had a lower transfer velocity than that predicted from the scaling relation.

The transfer velocity scaled with the 4/5 power of wind speed for all building surfaces (Fig. 7). Here, each regression line included the adjustment of the transfer velocity in calm conditions ($W_{t,\mathrm{calm}}$). The magnitude of $W_{t,\mathrm{calm}}$ is 0.005 m s^{-1} for the wall surfaces and 0.007 m s^{-1} for the roof surface. For a street surface in a 2D canyon, Barlow et al. (2002) asserted that there is a linear dependence between transfer velocity and wind speed (U_∞); namely, transfer coefficient (W_t/U_∞) is independent of Reynolds number. From the viewpoint of urban climate modelling, this simple relation is useful and convenient because the dimensionless transfer coefficient can be determined for a given street geometry regardless of wind speed. Our result is not in agreement with the linear relation, but the deviation from linear relation is not large in practice. So our result does not completely deny the possibility of assumption of this convenient linear relation in reality. But within the range of wind-tunnel scale model experiments, the scale effect is too large to be neglected. Hence, in the

following analyses, the comparison in each figure is restricted to data from the same size sample.

4 Results

4.1 Two-dimensional street canyon models

Setting the cubic model between long rectangular models, we made an array of 2D street canyons (Fig. 8). The sampling area was positioned laterally in the centre of the wind tunnel. Here, the model height H is constant for all cases, and the different canyon shapes were generated by adjusting the width between models W from 5 to 450 mm. As indicated in Fig. 6, the change of model height has a rather complex effect due to the deviation of the vertical mean wind profile near the surface. This is the reason we decided to keep the model height constant. Therefore, in our study the canyon shape is described using an aspect ratio of W/H (canyon width normalized by constant height), not the commonly used H/W. Consequently, the canyon aspect ratio in this experiment ranges from 0.083 (= 1/12) to 7.5. The wind direction was always perpendicular to the street.

Figure 9 shows streamwise variations of transfer velocity for typical aspect ratios. In Barlow and Belcher (2002) and Barlow et al. (2004), the transfer velocity of the street surface was also analyzed as well as that of the wall and roof surfaces. In our study, however, the street surface was not included because it is not clear how the different sample sizes of the street can be compared to the other surfaces. In all surfaces, the value in the first canyon is larger than those downstream and the values equilibrate within $X/H = 7$–10 from the leading edge. The decreasing rate is more rapid for the narrower canyons. Although such an adjustment length has been compared with the number of canyons in many studies, it is preferable to describe this with the distance normalized by the model height. The roof value is always larger than that of both kinds of wall surfaces. Also, the windward wall is sensitive to the aspect ratio; its value is close to that of the leeward wall for $W/H = 1/2$ and close to the roof surface for $W/H = 2$.

Next, using the data in the uniform-value region near $X/H = 18$, the relations between mass transfer velocity and canyon aspect ratio were investigated (Fig. 10). The experiments were done at wind speeds of 2, 4, and 6 m s^{-1}. Because W_t/W_{t0} variations as a function of aspect ratio were almost the same at all wind speeds (not shown here), their averaged values for each surface type are shown in this figure. The transfer

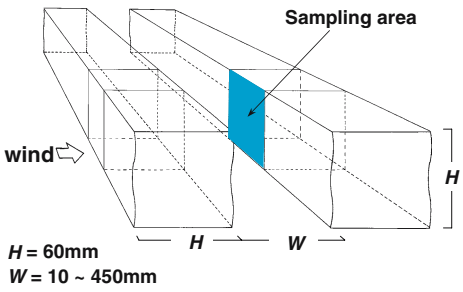

Fig. 8 The 2D canyon model and sampling area. The extent of the model setting area is 1500 mm (= 25H) in both lateral (crosswind) and longitudinal (along-wind) directions

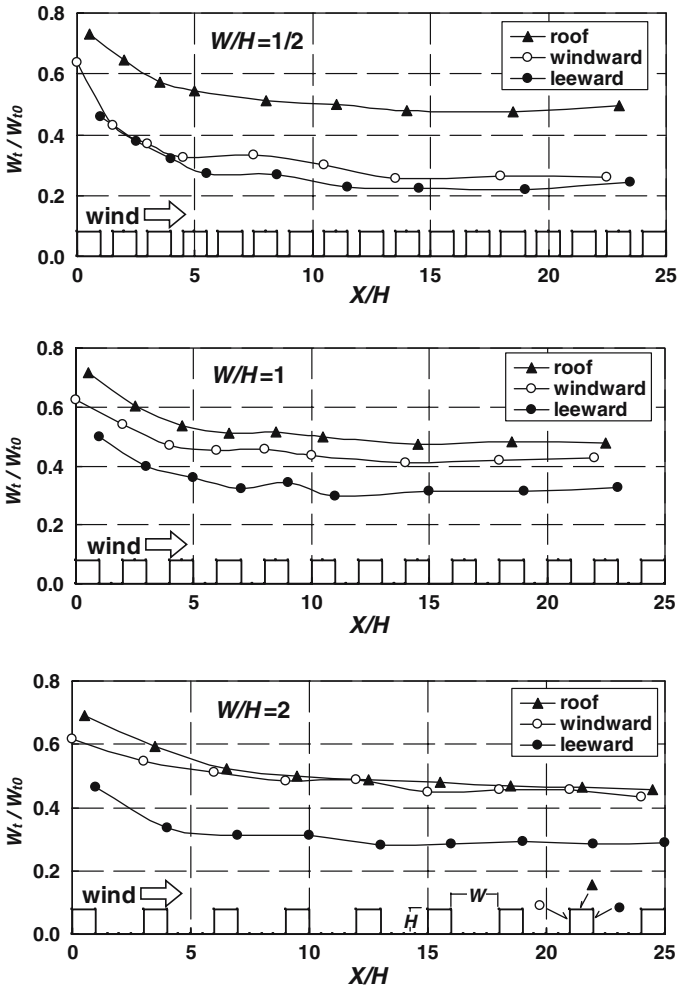

Fig. 9 Streamwise variation of the normalized transfer velocity on 2D canyon surfaces for three values of W/H

velocity of the leeward wall is about 2/3 that of the windward wall in the range of sufficiently large aspect ratio (W/H). According to Oke's (1998) classification scheme, this is called *isolated roughness flow*. For the windward and leeward walls, there is a clear decrease in the transfer velocity with aspect ratio in $W/H < 1$, and they converge to the same value for $W/H \ll 1$ (*skimming*). In the range of $1 < W/H < 2.5$, the leeward wall has a local peak whereas the windward wall decreases, a behaviour that indicates the development of vortex flow in the street canyon. This range corresponds to the flow regime of *wake interference*. On the other hand, the roof value changes little except for a slight decrease for $1 < W/H < 2.5$. This dip in the roof value agrees with the result of Barlow et al. (2004) obtained using the naphthalene sublimation method, but it differs from our result in that the windward value does not exceed the roof value at this aspect ratio. In addition, the appearance of the peak in the leeward

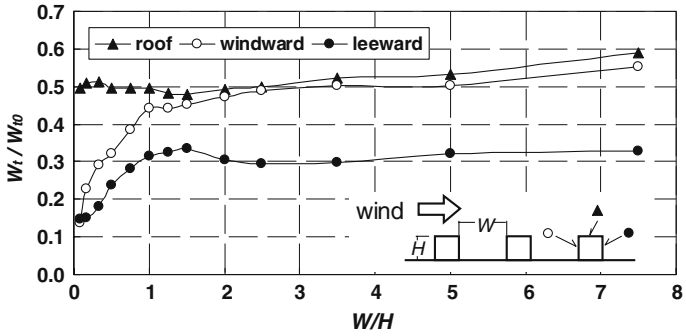

Fig. 10 Normalized transfer velocity for 2D canyon surfaces for a range of canyon aspect ratios *W/H*

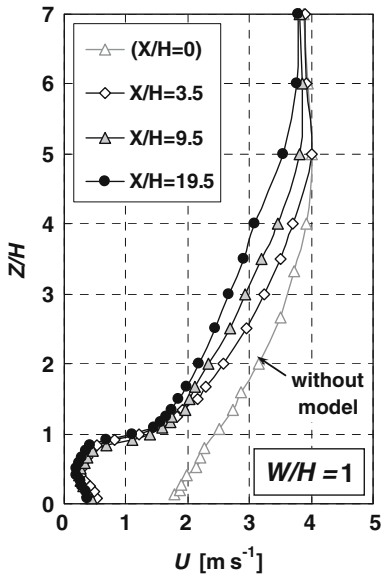

Fig. 11 Change of the mean wind profiles at the centre of 2D canyon along the wind direction ($W/H = 1$)

surface within the wake interference zone and the tendency for monotonic decrease in the windward surface are also in agreement with their results.

In Fig. 11, we show the change of mean wind profiles at the canyon centre along the wind direction ($W/H = 1$). To reveal the magnitude of the decrease in wind speed concerning this open wind tunnel, the wind speed is expressed without any normalization. In comparison with the approaching profile at the start of the working section, the mean flow above the top of the boundary layer decreases about 3% at the end of the working section due to the divergence of air flow in the open circuit. Though the boundary layer for the 2D canyon array also develops along the wind direction, the flow pattern within the canyon is almost constant in the W_t equilibrium region.

4.2 Effects of an additional wet surface in the 2D street canyon

Barlow et al. (2004) showed the influence of an additional in-canyon source on the transfer from each surface. In general, an additional source increases the concentra-

tion of scalar within the canyon. The transfer from each surface is inhibited by this increased concentration; however, the amount depends on the aspect ratio and the surface position within the canyon. Thus, the results of experiments with such an additional source are useful to understand the flow characteristics and ventilation rate of the street canyon.

For the experiments, we expanded the wetting surface laterally to the full width of the 2D canyon. Then, we examined the decreasing rate of transfer velocity of each surface by additional wet surfaces for various canyon shapes. The sampling area was 60 mm wide, same as the experiments in the previous section. Figure 12 shows the results for $W/H = 1$. In all three surfaces, the normalized transfer velocity decreased when an additional wet surface was added.

For the transfer velocity of the windward wall, the effects of leeward wall wetting and street surface wetting are only 3% and 6%, respectively. Even when both additional surfaces were wet, the decrease was only 14%. Such insensitivity means that the above fresh air flows efficiently near the windward wall and so the transfer velocity is unaffected by the increase of water vapour concentration within the canyon. On the other hand, the additional wetting has a considerable influence on the transfer velocity of the leeward wall; a 20% decrease in the double wetting cases and a 35% decrease in the triple wetting case. For this aspect ratio, vortex flow is developed within the canyon and thus the wetting of the windward wall and street surface caused large increases of water vapour concentration near the leeward wall. In Barlow et al.'s (2004) double source experiments, the decrease of the transfer coefficient by adding a street source is larger on the windward wall than on the leeward wall for $H/W = 1$. This differs from our results in Fig. 12. For the street surface, wetting of the windward wall greatly decreased the transfer velocity (-23%), as it also reduced the leeward wall value (-20%). In contrast, the effect of leeward wall wetting is relatively small (-9%) because the leeward wall is downstream of the street in vortex flow. This finding also contrasts with Barlow et al.'s (2004) result for the transfer coefficient of a street surface with $H/W = 1$; the effect of an additional source on the windward wall was the same as that on the leeward wall.

Figure 13 shows the changes in the transfer velocity of the windward and leeward walls by wetting the opposite facing wall. The changing ratio is the value for the two-wall-wet case divided by the single-wall-wet case. For the windward wall, the effect of leeward-wall wetting is small and is nearly independent of the aspect ratio. For the leeward wall, there is a significant reduction in transfer velocity for $W/H > 1/3$. For the narrowest street ($W/H = 1/6$), the effect of additional wetting is small because the water vapour concentration within the canyon is sufficiently high even for single wetting. As a whole, the effects from the additional wetting are consistent with the expected flow patterns.

4.3 Distribution within a surface for the 2D street canyon

An advantage of this method is the ease with which the flux can be restricted to be within an arbitrary surface. By cutting the filter paper into a 10-mm strip, the distributions within each surface could be studied for the 2D street canyon. Figure 14 shows the building model for such a 'split measurement', and the sampling area. The measurements were done the same way as the whole surface measurement in Section 4.1, but the wet surface is now only part of sample paper (10×60 mm). By shifting the location of the wet region on a surface, we determined the transfer velocity dis-

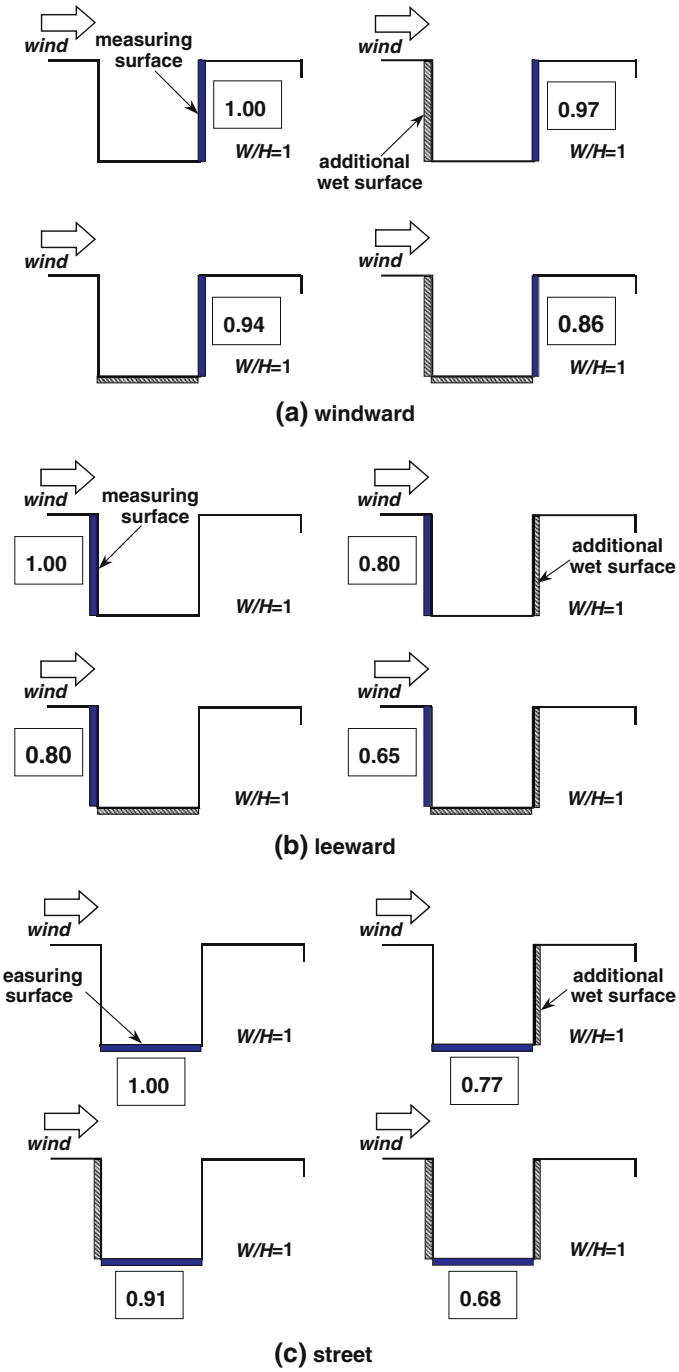

Fig. 12 Normalized transfer velocity without (upper left) and with (others) an additional wet surface in a 2D canyon for $W/H = 1$; (**a**) windward wall, (**b**) leeward wall, (**c**) street surface

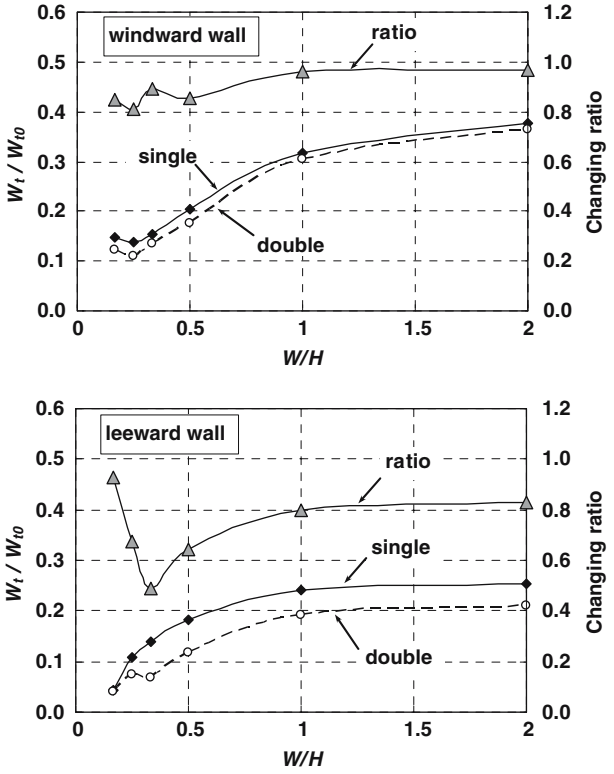

Fig. 13 Normalized transfer velocity for 2D canyon surfaces with an additional wet surface for various aspect ratios *W/H*. 'single' means that only the measuring surface was wet, 'double' means that the opposite facing wall was also wet. The changing ratio is the ratio of the double value to the single value

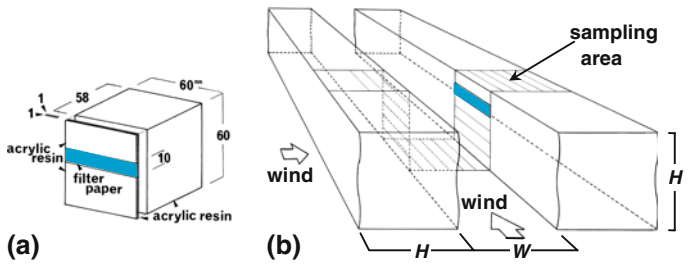

Fig. 14 (**a**) Sample of building model for split measurement. (**b**) Schematic view of two-dimensional canyon model and sampling area for split measurement

tribution over the canyon surface. In addition, we could determine the street surface transfer velocity because the sample size could be kept the same as that on the roof and wall surfaces. The shape and dimension of the upstream reference sample was the same as that in the whole surface measurements so that we could compare the W_t/W_{t_0} value of this split measurement with that of the whole surface measurements.

The results for various canyon shapes are shown in Fig. 15 for the perpendicular wind direction. For the narrowest streets, which are in the *skimming flow* regime ($W/H = 1/6$), the distribution for the leeward wall is similar to that of the windward wall. Baik and Kim (1999) found a two-vortex flow regime for $W/H < 1/2$ using a numerical model with k–ε turbulent closure scheme. But the result of having such a symmetrical distribution is that there is no clear flow pattern within the canyon. As the canyon widens, the transfer velocity in the upper part of the windward surface increases sharply. For the windward wall, the transfer velocity always increases with height. In contrast, the distribution on the leeward wall has a peak in the middle of the surface in the case of $W/H = 1$ and 3/2. For the street surface, a peak in the transfer velocity always occurs, except when $W/H = 1/6$, due to the vortex flow within the canyon. And the transfer velocity decreases clearly in the street canyon corners where the flow separates. For the roof, the transfer velocity decreases slightly in the downstream direction in all cases.

In the lower part of Fig. 15, we combine the distributions for all surfaces. Harman et al. (2004) proposed a model for the transfer velocity distribution within a 2D canyon, based on a wind speed model in the recirculation region in which the airflow decelerates exponentially as it travels around the canyon. However, the data in Fig. 15 show that the local transfer velocity does not decrease monotonically from first impingement position along the recirculation stream line, even in the cases in which the recirculation flow pattern clearly exists. Regardless of the canyon aspect ratio, the peak velocity in the street is at the same distance from the windward wall: about one-half of the model height. It can be interpreted as the impingement region of recirculation flow on the street. For the windward wall, the transfer velocity generally increases with street width until $W/H = 3/2$; however, it is almost constant for a wider canyon. As for the bottom part of the windward surface and the adjacent part of the street surface, W_t is also constant for W/H exceeding 3/2. It is inferred that the flow into the canyon does not change largely for $W/H > 3/2$. In contrast, the distribution for the leeward wall is more complicated. Although it is almost uniform near the top, it has a clear peak a little below the mid-height for the cases $W/H = 1$ and 3/2. The peak position remains at about $0.4\,H$ from the street, a behaviour that is similar to the peak on the street. On the roof, the transfer velocity slightly increases as the street width decreases, because the flow near the roof surface accelerates shifting to a skimming flow pattern.

In urban climate modelling, the simplest way to assign wall transfer velocities is to assume the same value for all positions on a wall, depending on the aspect ratio. From Fig. 14, we can deduce the relative variation when the average of all points on both the windward and leeward walls is assumed for both wall surfaces. On the windward wall, the relative variation is largest at the top, with more than 100% underestimation in some cases; for the leeward wall, the transfer velocity is overestimated for most cases.

When the wind is along the street direction, the distribution of transfer velocity is nearly symmetrical (Fig. 16) and the minimum values are near the bottom corners, similar to the cross-street wind direction cases. The transfer velocity increases with height along the walls and it has a gentle peak in the middle of the street. On the roof, the distribution of transfer velocity is nearly uniform, and its value is slightly larger than that of the top of the walls.

A comparison of the transfer velocity between these split measurements and the whole surface measurements is helpful for understanding the flow regime within the

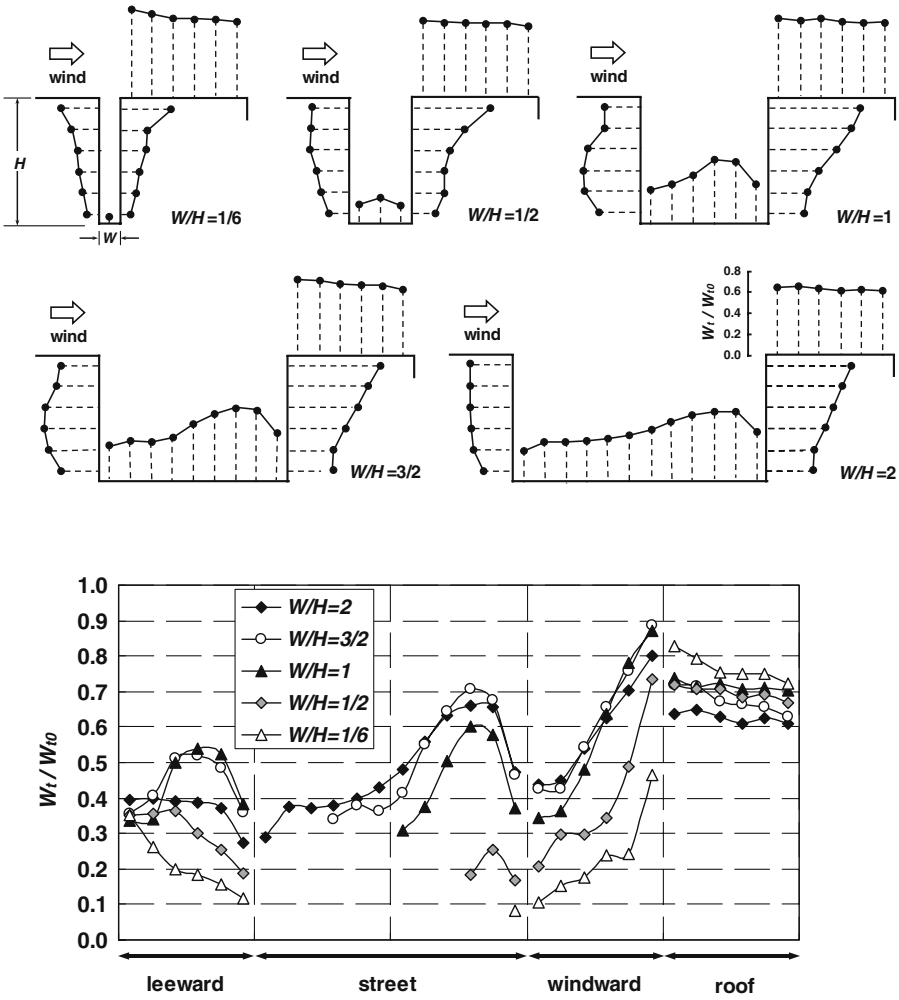

Fig. 15 Distributions of normalized transfer velocity for all surfaces in a 2D canyon for various aspect ratios. The wind was perpendicular to the street direction

Fig. 16 Distributions of normalized transfer velocity for all surfaces in a 2D canyon for $W/H = 1$. The wind was parallel to the street direction

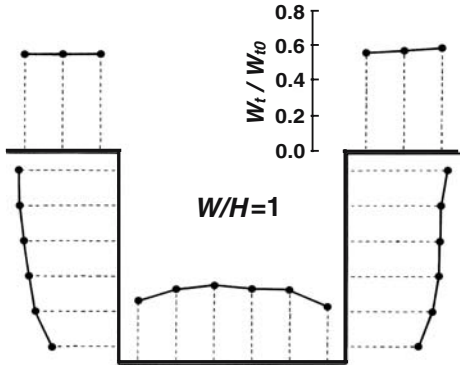

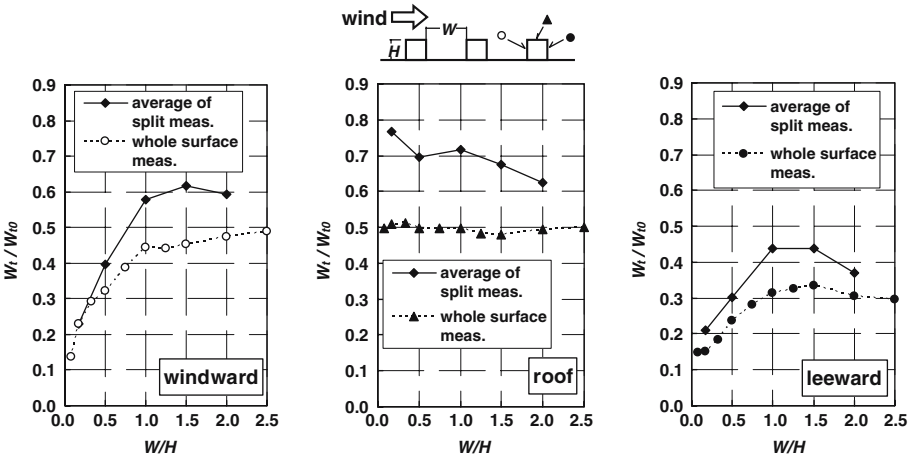

Fig. 17 Normalized transfer velocity from whole surface measurements and the average of split measurements in 2D canyons of various *W/H*

canyon. We calculated the averages of the six split samples on a given surface and then compared these to that of the whole surface measurement (Fig. 17). In general, the average of the split measurements is larger than the whole surface measurement because of the edge effect described in Section 3. The amount of increase depends on the canyon shape (*W/H*) and the surface type. In extremely narrow canyons, the increase in transfer velocity for the splitting sample is very small for both walls, and suggests that there is no clear flow pattern along the surface for such a small *W/H* condition. In contrast, there is a large difference between the measuring methods when the vortex flow occurs within the canyon, namely when *W/H* is between 1 and 3/2. On the roof surface, this difference decreases with canyon width; therefore, the edge effect is particularly noticeable in the skimming flow regime. As the canyon widens, flow separation at the top of the windward wall increases the turbulence intensity near the roof surface. That is the reason why the edge effect is relatively ambiguous at large *W/H*. Assuming a $-1/5$ power law (e.g. Fig. 6), the scale down of the sampling area by a factor of six should result in about a 43% increase in transfer velocity; that is $(1/6)^{-1/5} = 1.43$. This roughly agrees with the results for the walls with $W/H = 1$ and 3/2 and for the roof. In these cases, a 'cleaner' internal boundary layer may be developing along the surface.

To infer the contribution rate of each surface, we show the averaged transfer velocity normalized by roof transfer velocity for a perpendicular wind direction (Fig. 18). In Barlow et al.'s (2004) results, the windward transfer velocity exceeded that of the roof surface for $W/H = 1.6$. In addition, their mean ratio of the transfer velocity for windward and leeward walls is generally larger than our results. There is a difference in method between our 'split' measurement and their approach with a 'whole' surface source. Is that the main reason for this discrepancy in the normalized transfer velocity $(W_t/W_{t_{\text{roof}}})$? As for the results in Figs. 15 and 17, we would obtain different 'absolute' values if we choose a different split measurement, for example 1/3 or 1/10. In this sense, these results are not quantitative but qualitative. Then, in Fig. 18, we also plot the result of our 'whole' surface measurement for the windward and leeward walls.

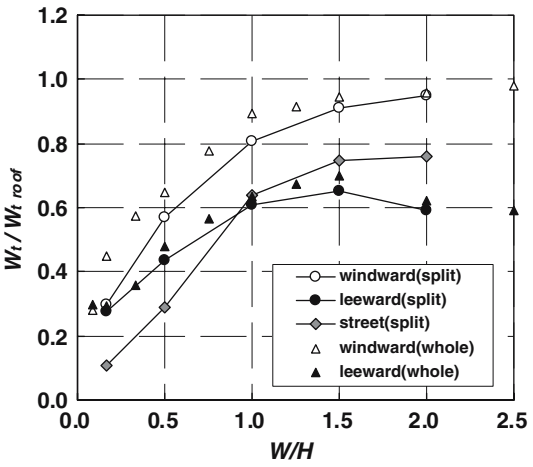

Fig. 18 Transfer velocity for each surface of a 2D canyon normalized by roof transfer velocity. The wind was perpendicular to the street direction

The difference in this 'relative' value of transfer velocity is fairly small between the 'split' measurement and the 'whole' surface measurement.

4.4 Three-dimensional cubic array

Studies of 2D urban canyons are useful for gaining a fundamental understanding of urban areas; however, 3D experiments are needed to fully understand the behaviour of the transfer velocity in real urban areas. For example, using a large-eddy simulation, Kanda et al. (2004) found systematic turbulent structures above a 3D city-like setting. Here, as a first step towards describing the 3D structure, the change of transfer velocity due to building density was investigated for simple uniform cubic arrays. The area of the model setting is 1500 mm ($= 25\,H$) both lateral and longitudinal, similar to the 2D canyon experiments.

We start by examining the longitudinal variations of transfer velocity along the cubic array, shown in Fig. 19 for the same W/H values as used in the 2D case (Fig. 9). The adjustment region is smaller than that for the 2D case, and it is hard to discern in the sparsest arrangement. The steep decrease of the transfer velocity occurs within $X/H = 4$ to 5 from the leading edge, indicating that the drag distribution of a 3D canopy allows more rapid flow equilibration.

Next, we examine the region near $X/H = 18$, where the transfer velocity does not change with X. In sufficiently sparse conditions, the roof has the highest transfer velocity, followed by the windward wall, then the sidewall, and the leeward wall (Fig. 20). The roof top value decreases gradually as the building density increases; accordingly, in the range of $1 < W/H < 5$, the windward wall has a highest value among all surfaces. Such a significant change of the roof top value is very different from that of the 2D case. In the range of $W/H < 1$, the roof top value is almost the same as that of the 2D street canyon. Another point is that the value for the leeward wall does not change until $W/H < 1$, whereas that of other surfaces begins to decrease near $W/H = 5$. In the 3D case, the leeward wake region is strongly affected by the flow around the building side wall. This flow resulted in another distinct difference—that there is no local peak near $W/H = 1$ and 3/2 due to the vertical vortex between obstacles as occurred in the 2D street canyon case. In other words, the turbulent condition near

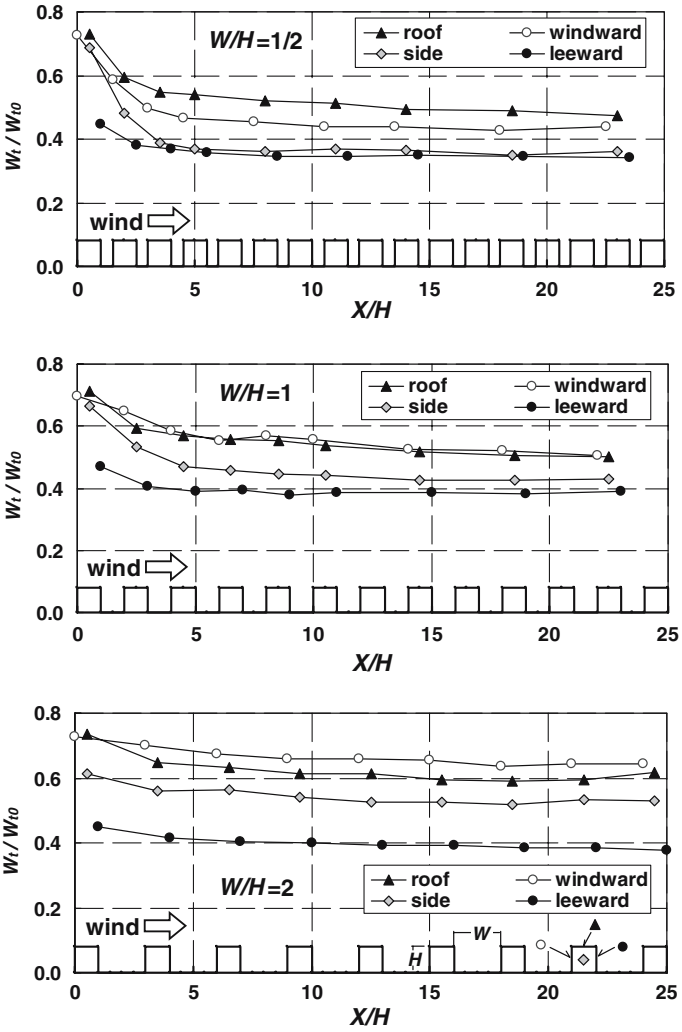

Fig. 19 Normalized transfer velocity along the wind direction for regular cubic arrays

the leeward wall is almost constant except for the very dense condition: $W/H < 1/2$. For the sidewall, its value is close to that for the leeward wall in dense conditions; however, it is close to that for the windward wall in sparse settings.

4.5 Transfer velocity dependence on wind direction in a 3D array

In this section, we describe how the wind direction affects the transfer velocity in a 3D setting. First, the results of a single cubic model for every 7.5 degrees are shown in Fig. 21. Here, the value of the transfer velocity is normalized to that for the right angle wind direction case. As for the wall value, the maximum peak appears not at the right angle but near $\theta = 10$ degrees. Another peak is near $\theta = 75$ degrees, and the

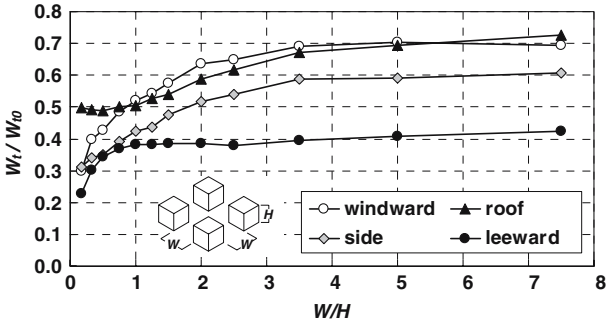

Fig. 20 Normalized transfer velocity for a regular cubic array as a function of aspect ratio *W/H*

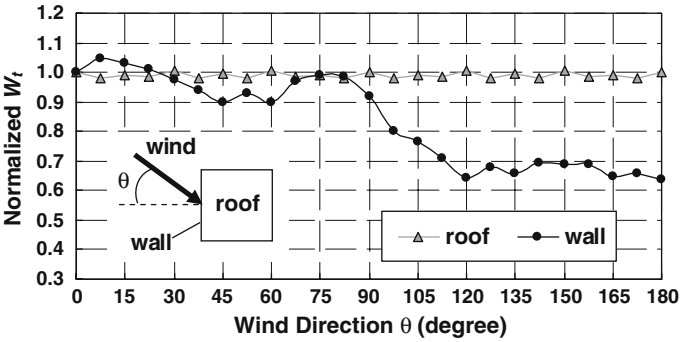

Fig. 21 Transfer velocity of the single cubic model for various wind directions. The value of transfer velocity is normalized to that for $\theta = 0$

value decreases sharply until $\theta = 120$ degrees, then it shows an almost constant value to the end. In contrast, the roof surface is uniform within ±2%.

We now consider more complicated settings. Figure 22 shows the model arrangement used to study the transfer velocity dependence on wind direction. By placing four cubic models together, we made the rectangular building model of 1:1:4 proportions, and the models were set so that all intervals between models were equal to the model height H. Accordingly, the building coverage ratio λ_p equals 0.4. The reason why we chose cuboids in the ratio 1:1:4 rather than cubes is to study the effect of street length on transfer velocity under a constant aspect ratio. Besides we intended to check the magnitude of the spatial variation in transfer velocity for a rather complex structure. Each sampling area is square with dimensions 60 × 60 mm, and there are 20 sampling positions: 4 roof surfaces (R), 10 wall surfaces (B, F, and S), and six street surfaces (G and G′). These surfaces cover one iterative structure unit such that the array is composed of only these units. The average transfer velocity over these 20 surfaces should represent this model arrangement. In the experiments, only one square surface is wet and the measurements were done for the five wind directions: $\theta = 0$, 22.5, 45, 67.5, and 90 degrees.

Figure 23 shows the results for all surfaces and wind directions. The transfer velocity is normalized by the average of all data (= 20 surfaces × 5 wind directions). For the right-angle case ($\theta = 0$ degrees), the transfer velocity is larger on both ends of the

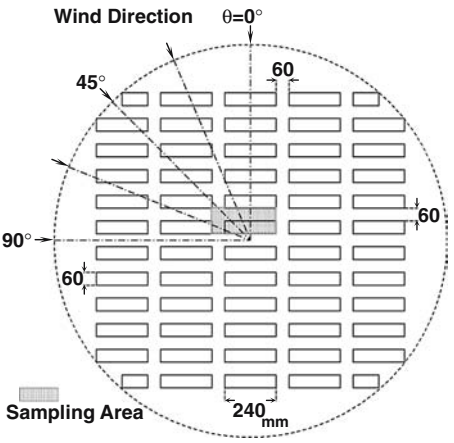

Fig. 22 Model arrangement and sampling area to determine how the transfer velocity depends on wind direction

windward wall, but it is larger in the centre for the leeward wall. The latter phenomenon results from the vertical vortex flow between the buildings. For the same reason, the transfer velocity for the street surface between buildings (G) is larger than that of the street surface parallel to the wind direction (G′). The large W_t values on the roofs of the end blocks are probably due to end vortices, which recirculate the drier air in the environment onto the roof. As θ increases, the tendency for downstream directions to have lower transfer velocities becomes clear for walls, roof, and the street parallel to the buildings. Such a decrease of W_t in the along-wind direction is quite obvious and systematic for the 90 degrees wind direction. Since the wetted surface is only measuring a square surface in each case, these decreasing W_t distributions are not due to the edge effect. Therefore, this results from the fact that turbulence is produced around the intersection and diminishes along the wind direction until the next intersection. The largest variation due to wind direction is on the S-wall (the short side wall), particularly on the side facing the wind.

The 2D distribution pattern can be seen only in the right-angle ($\theta = 0$ degrees) case within the canyon formed between long buildings. In other words, the airflow was channelled along the canyon for most wind directions, in contrast to the vertical vortex flow that is characteristic of a 2D canyon. Even in the perpendicular wind direction, the horizontal separation flow at both ends of the building significantly affected the transfer velocity distribution.

In Table 2, the spatial average and the magnitude of the deviation are listed for three surface types: roof, wall, and street. These data were expressed as a normalized transfer velocity by the area-average over all wind directions; therefore, we can deduce the deviation from this table when a certain uniform value is used for all surfaces independent of wind direction. Locally, the deviations range from 1.48 to 0.71. However, the variation of total average of all surfaces due to wind direction is relatively small, ranging from 0.92 to 1.06. For this arrangement, the roof has the highest transfer velocity, followed by the wall, then the street for all wind directions.

To estimate the contribution rate for each surface type at a given angle, the transfer velocity normalized by the area-average for each wind direction is shown in Table 3. From these values, one can determine the deviation when the spatially averaged value is given for all surfaces at a given wind direction. In this case, local deviations slightly

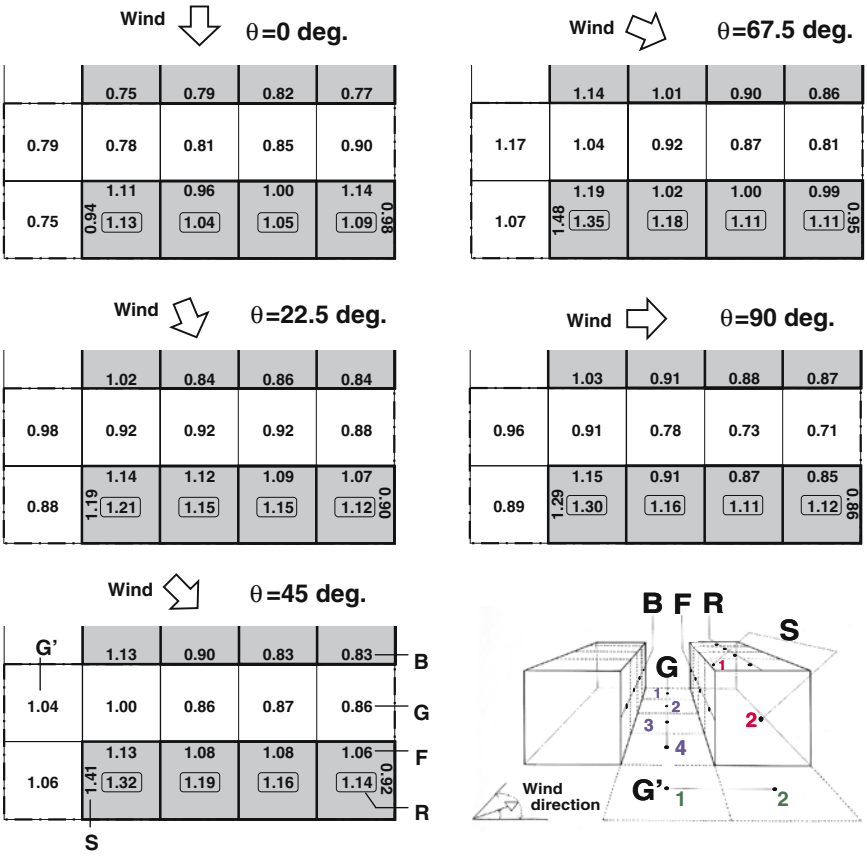

Fig. 23 Normalized transfer velocity W_t/W_{t_0} of each surface region for various wind directions. The view is from above and the values near the edge are for walls

Table 2 Normalized transfer velocity in each type of surface for various wind directions

Type of surface	Area (lot=100)	Normalized (W_t/W_{t0}) by the total average					
		Wind direc.	0	22.5	45	67.5	90
Roof (R)	40	max.	1.13	1.21	1.32	1.35	1.30
		ave.	1.08	1.16	1.20	1.19	1.17
		min.	1.04	1.12	1.14	1.11	1.11
Wall (B+F+S)	100	max.	1.14	1.19	1.41	1.48[a]	1.29
		ave.	0.93	1.01	1.04	1.05	0.96
		min.	0.75	0.84	0.83	0.86	0.85
Street (G + G′)	60	max.	0.90	0.98	1.06	1.17	0.96
		ave.	0.81	0.92	0.95	0.98	0.83
		min.	0.75	0.88	0.86	0.81	0.71[b]
(Total)	200	Ave.	0.92	1.01	1.04	1.06	0.96

Symbols R, B, F, S, G, G′ are defined in Fig. 22. The values mean the ratio of transfer velocity to the average for all types of surface and all kinds of wind direction (20 surfaces × 5 wind direction). [a] the maximum value; [b] the minimum value.

Table 3 Normalized transfer velocity for each type of surface and range of local variation in each wind direction

Type of surface	Normalized (W_t/W_{t0}) by the average for each wind direc.						
	Wind direc.	0	22.5	45	67.5	90	ave.
Roof	ave.	1.17	1.15	1.15	1.12	1.22	1.16
Wall	ave.	1.00	1.00	0.99	1.00	1.00	1.00
Street	ave.	0.88	0.91	0.91	0.93	0.86	0.90
Range of variation	max./Ave.	1.24	1.20	1.35	1.40[a]	1.34	1.31
	min./Ave.	0.81	0.83	0.80	0.76	0.74[b]	0.79

The values mean the ratio of transfer velocity to the average for all types of surface in each wind direction (each 20 surfaces). [a] the maximum value;

[b] the minimum value.

decrease from Table 2 and range from 1.40 to 0.74. The value for the wall is close to 1.0 for all angles (from 0.99 to 1.00), which means that the wall-averaged transfer velocity is equivalent to the area-averaged value for all wind directions. Although the averaged values change from 1.12 to 1.22 for the roof and from 0.86 to 0.93 for the street, the contribution rate for each type of surface to the transfer velocity is insensitive to wind direction. As for the average of all wind directions, the transfer velocity is about 16% larger for the roof, and about 10% smaller for the street, than the area-averaged value that is nearly equal to the wall surface.

4.6 Effects of spatial heterogeneity

Studies using periodic arrangements provide useful information, but real cities are more complex. As a step to approaching a more realistic city layout, we investigated the transfer velocity for a cluster block array surrounded by relatively wide streets. The basic cluster consists of 25 (5×5) cube models and had a plane area building density λ_p of 0.73 and an aspect ratio $W/H = 1/6$ (Fig. 24, type-A). We set 9 clusters (3×3) in a working section, and measured the distribution of the transfer velocity about the central cluster. The street aspect ratio between each cluster was set to $W/H = 1$.

Figure 25 shows the variations of transfer velocity in longitudinal and lateral directions. Because the cluster is created intentionally as a dense block, there is a significant difference between the core zone and the peripheral zone. The maximum value is at the windward wall facing the wide street near the intersection and the minimum value is in a leeward surface in the core region. The difference between them is about a factor of two. Even the side and leeward walls, the outer façade facing wide streets, is about 70% larger than that in the core section. Within the core section, the difference due to the wall orientation is less than 20%. On the roof, the values are almost uniform over the cluster and, except for the outer façade, are nearly twice as large as those of the walls.

Using this cluster array, we then examined the influences of a different city structure in the middle of each cluster. In Fig. 24, type-B has the centre building removed, thus creating an open space; type-C has a building of a different height in the middle. In type-C, the building volume was fixed because the dimension of the modified cuboid model is half of the cubic model in horizontal area and twice in height. The ratios of the transfer velocity to the corresponding value on the type-A model are shown in Fig. 26.

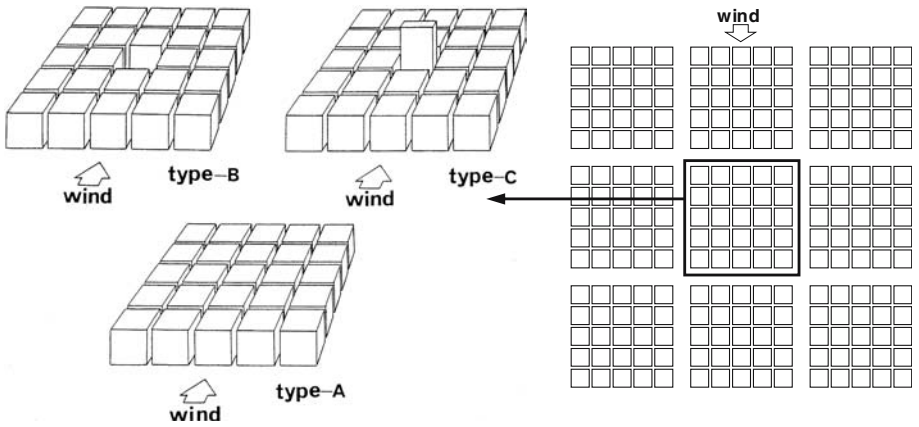

Fig. 24 Model arrangement with spatial heterogeneity. Aspect ratio within each cluster is $W/H = 1/6$ and the gap between the building clusters is equal to model height. For type-C, the centre building had twice the height of the other buildings but the same volume

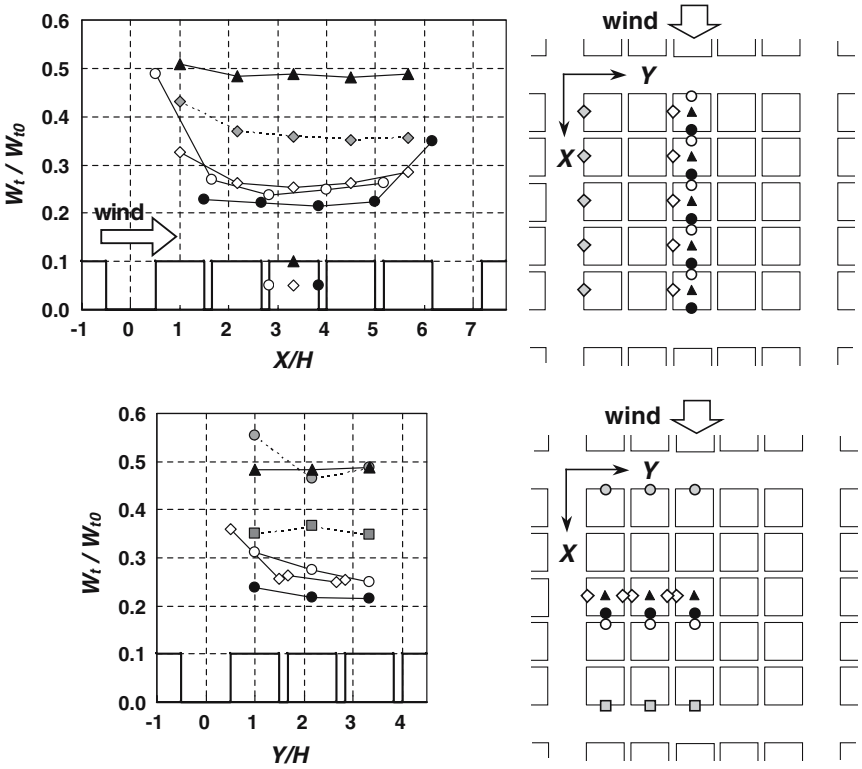

Fig. 25 Longitudinal and lateral distributions of normalized transfer velocity in the type-A arrangement of Fig. 24. The symbols in the plots are located in the positions shown in the sketches at right

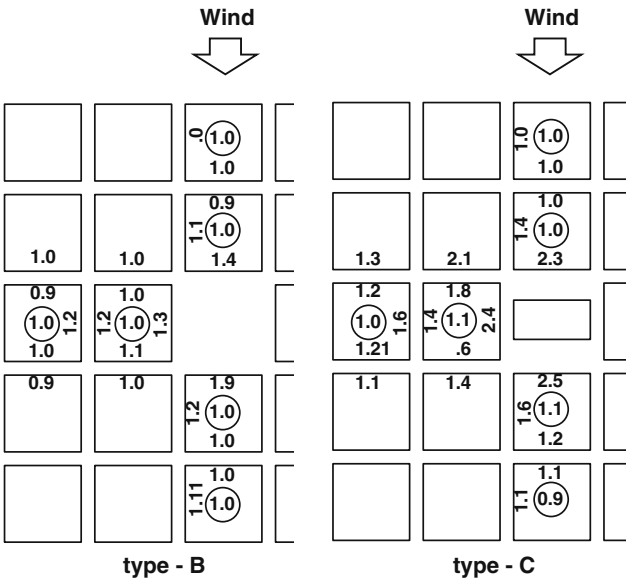

Fig. 26 Ratios of the transfer velocity in a given position of types B or C to the type-A value. Left side is for the type-B case in Fig. 24. Right side is for the type-C case in Fig. 24. Circled number means the value on the roof

By removing the centre cubic model, the transfer velocity increases significantly on the wall surfaces around the open space. These changing ratios can be explained nearly by the results of regular cubic array shown in Fig. 20. Whereas laterally, the effect extends to the narrow path next to the open space, longitudinally the variation is restricted to within the open space. Also, no difference is discernible for the roof. However, the effect of building height heterogeneity is significant. In spite of the slight change concerning only one building, the transfer velocity increases throughout the cluster except for the first (top) array in the cluster. This is because the double-height building entrains air with higher wind speeds from a higher level and increases ventilation rates of street canyons. In urban climate modelling, a complicated city structure sometimes has been modified to the equivalent regular cubic array. However, this case indicates that models with uniform height arrays significantly underestimate the area-averaged transfer velocity.

5 Conclusions

The water evaporation technique was developed to study the transfer velocity on urban surfaces. In this technique, the scale effect was too large to neglect, especially when the sample size was less than 100 mm. According to the dimension-change experiments, the surface-averaged mass transfer velocity was proportional to the $-1/5$ power of length of the sample along the wind direction, suggesting that the local transfer velocity was proportional to the 4/5th power of the Reynolds number. The results for several wind speeds supported this Reynolds number dependency. Because of this scale dependence, we derived all conclusions on the basis of data from

samples of the same size. About this Reynolds number dependency, however, there is room for further investigation to determine its adaptable scale limit. According to the review of Hagishima et al. (2005), there is no conclusive proof that such a scaling law holds over the full range of Reynolds numbers up to the order of 10^6 or 10^7 at full scale. Therefore, we focused on the 'relative' values of local transfer velocity and its variation due to canyon geometry and wind direction. The reason why we take such a strategy is that these relative values are expected to be robust and irrespective of measuring method and scale.

For 2D canyons, the transfer velocities from roof and wall surfaces were analyzed in the downstream region where the values did not depend on their absolute position (equilibrium region). The windward-wall transfer velocity showed a general decrease with decreasing aspect ratio W/H, whereas the transfer velocity of the leeward wall had a slight peak for $1 < W/H < 2$, which is in the wake interference flow regime. In this flow regime, the roof transfer velocity slightly decreased, but its variation was less than 10%.

The transfer velocity distributions within each surface were also revealed using the split measurements. The local transfer velocity decreased around both street corners, and had a peak on both the leeward wall and street surfaces for a fixed aspect ratio. Therefore, the transfer velocity did not monotonically decrease along the canyon surfaces, although it increased gradually with height on the windward wall. Because of such a complex dependence of transfer velocity on positions within wall surfaces, if one parameterized the wall transfer velocity only by the canyon shape, large local errors would occur in some cases. Including the distribution of sunlit or shaded parts within the wall surfaces, the neglect of these transfer velocity variations would cause considerable error for predictions of area-averaged heat fluxes.

What is an important point and has been clarified from the comparison between split measurement and entire surface wetted approach is the dependency of the scale effect on flow pattern. There is no doubt about the fact of the scale effect for horizontal surfaces where a clear internal boundary layer is developing. However, if there is no obvious parallel flow along the surface, the scaling law for a horizontal surface may not hold for such kinds of surface. This is another reason why we focused on the 'relative' values of local transfer velocity. The evidence that relative values are robust and irrespective of scale can be seen in the transfer velocity normalized by the roof transfer velocity.

As with the 2D canyon case, the transfer velocity for a 3D cubic regular array was analyzed in the equilibrium region as a function of aspect ratio. The dependency of transfer velocity on aspect ratio was considerably different from that of a 2D canyon. There was no peak in the leeward wall in the wake interference flow regime, and the transfer velocities for roof, side, and windward surfaces began to decrease gradually with decreasing aspect ratio for $W/H < 5$.

The wall transfer velocity dependency on wind direction for the single cubic model was measured in detail. A variation in wind direction by only a few degrees could drastically change the wall transfer velocity. In leeward conditions, however, the transfer velocity was almost constant over the range of ± 120 degrees wind direction, or about 2/3 of the windward wall magnitude.

A similar wind-direction dependency was examined for the 3D city-like setting. This case-study setting included canyon space between elongated buildings four times longer than their width and height, and the streets were as wide as the buildings were tall. The area-averaged transfer velocity was not sensitive to wind direction changes:

less than ±8% of the average over all wind directions. Nevertheless, the local variation of transfer velocity was considerable: from 0.71 to 1.48 of the average over all wind directions for the examined model arrangement. Except for only the cross-canyon wind direction case, the flow tended to channel through the canyon, and the transfer velocity generally decreased along this channel flow. Though it could not be treated in the present work, fluctuations of wind direction in natural wind are an important factor for understanding the behaviour of transfer velocities in urban areas. That is the problem that we have to consider next, and field experiments using a scale model under natural wind conditions are desirable (Kanda et al. 2005).

Another case study was performed on the effect of spatial heterogeneity. Using a densely clustered block surrounded by relatively wide streets, we found that the transfer velocity in the core region differed from that in the peripheral regions of the cluster. Adding open space in the cluster centre caused a considerable increase in transfer velocity around the open area, and can be understood as arising from an increase in ventilation. When the cluster centre instead had a building twice as high as the others, there were even larger and more extensive increases in the transfer velocity. Although the case studied here was limited, it is clear that heterogeneity has a large effect on the transfer velocity. This subject needs more consideration especially regarding vertical variation of model height (Narita 2004).

It has been shown that water evaporation is an appropriate technique to use for quantifying the effects of urban structure on transfer velocity. All results in the current work were acquired with the condition of a local source, that is, only one surface within the entire model was wet. It is an important point that the boundary layer of a measured scalar (water vapour) does not develop as that for momentum. Therefore, the results of the present experiments should be considered as dispersion phenomena from a local source but not as heat transfer phenomena from heated urban surfaces throughout the area. As was shown in the comparison between split measurements and whole surface measurements, the difference between them had a complicated dependence on flow characteristics. Nevertheless, the systematic data from the present work may be useful for urban climate studies.

Acknowledgements This research was financially supported by CREST (Core Research for Evolutional Science and Technology) of JST (Japan Science and Technology Cooperation) and by Grant-in Aid for Scientific Research from the Ministry of Education, Science and Culture of Japan.

References

Baik J-J, Kim J-J (1999) A numerical study of flow and pollutant dispersion characteristics in urban street canyons. J Appl Meteorol 38:1249–1261

Barlow JF, Belcher SE (2002) A wind tunnel model for quantifying fluxes in the urban boundary layer. Boundary-Layer Meteorol 104:131–150

Barlow JF, Harman IN, Belcher SE (2004) Scalar fluxes from urban street canyon. Part I: laboratory simulation. Boundary-Layer Meteorol 113:369–385

Clear RD, Cartland L, Winkelmann FC (2003) An empirical correlation for the outside convective air-film coefficient for horizontal roofs. Energy Buildings 35:797–811

Cole RJ, Sturrock NS (1977) The convective heat exchange at the external surface of buildings. Building Environ 12:207–214

Goldstein RJ, Cho HH (1995) A review of mass transfer measurements using naphthalene sublimation. Exp Therm Fluid Sci 10:416–434

Harman IN, Barlow JF, Belcher SE (2004) Scalar fluxes from urban street canyon. Part II: Model. Boundary-Layer Meteorol 113:387–410

Hagishima A, Tanimoto J (2003) Field measurements for estimating the convective heat transfer coefficient at building surface. Building Environ 38:873–881
Hagishima A, Tanimoto J, Narita K (2005) Review of the experimental researches on the convective heat transfer coefficient of the urban surfaces. Boundary-Layer Meteorol 117:551–576
Incropera F, DeWitte D (1996) Fundamentals of heat and mass transfer, 4th edn. Wiley, New York, 981 pp
Ito N, Kimura K, Oka J (1972) A field experiment study on the convective heat transfer coefficient on exterior surface of a building. ASHRAE Trans 78:184–191.
Kanda M, Moriwaki R, Kasamatsu F (2004) Large Eddy simulation of turbulent organized structure within and above explicitly resolved cube arrays. Boundary-Layer Meteorol 112:343–368
Kanda M, Kawai T, Kanega M, Moriwaki R, Narita K, Hagishima A (2005) Simple energy balance model for regular building arrays. Boundary-Layer Meteorol 116:423–443
Kusaka H, Kondo H, Kikegawa Y, Kimura F (2001) A simple single-layer urban canopy model for atmospheric models: comparison with multi-layer and slab models. Boundary-Layer Meteorol 101:329–358
Loveday DL, Taki AH (1996) Convective heat transfer coefficients at a plane surface on a full-scale building façade. Int J Heat Mass Transfer 39:1729–1742
Martilli A, Clappier A, Rotach MW (2002) An urban surface exchange parameterisation for mesoscale models. Boundary-Layer Meteorol 104:261–304
Masson V (2000) A physically-based scheme for the urban energy budget in atmospheric models. Boundary-Layer Meteorol 94:357–397
Masson V, Grimmond CSB, Oke TR (2002) Evaluation of the town energy balance (TEB) scheme with direct measurements from dry districts in two cities. J Appl Meteorol 41:1011–1026
Narita K (2004) Effects of building-height heterogeneity on area-averaged transfer velocity in the street surface – wind tunnel experiments using salinity change technique. Proc of 5th Symposium on the Urban Environment. AMS, Vancouver, Canada
Oke TR (1998) Street design and urban canopy layer climate. Energy Buildings 11:103–113